



Nonparametric Control Charts for Monitoring Serial Dependence based on Ordinal Patterns

Christian H. Weiß & Murat Caner Testik

To cite this article: Christian H. Weiß & Murat Caner Testik (2023) Nonparametric Control Charts for Monitoring Serial Dependence based on Ordinal Patterns, *Technometrics*, 65:3, 340-350, DOI: [10.1080/00401706.2022.2157883](https://doi.org/10.1080/00401706.2022.2157883)

To link to this article: <https://doi.org/10.1080/00401706.2022.2157883>



© 2023 The Author(s). Published with license by Taylor & Francis Group, LLC.



View supplementary material [↗](#)



Published online: 03 Jan 2023.



Submit your article to this journal [↗](#)



Article views: 1108



View related articles [↗](#)



View Crossmark data [↗](#)



Citing articles: 1 View citing articles [↗](#)

Nonparametric Control Charts for Monitoring Serial Dependence based on Ordinal Patterns

Christian H. Weiß^a  and Murat Caner Testik^b 

^aDepartment of Mathematics and Statistics, Helmut Schmidt University, Hamburg, Germany; ^bDepartment of Industrial Engineering, Hacettepe University, Beytepe-Ankara, Turkey

ABSTRACT

We consider the problem of monitoring for the existence of serial dependence in real-valued and continuously distributed processes. These can exist when a process goes out-of-control. Besides, as many control charts are designed under the assumption of independent and identically distributed observations, the validity of this assumption needs to be checked. In the literature, the majority of studies handled this problem by using a specific case of autoregressive moving-average time series models. Also a moving-window approach is often considered, which leads to the drawback that at least a window length of observations need to be collected before an out-of-control situation can be detected. Here, we use ordinal patterns and propose charts that are fully nonparametric and distribution-free, have a unique chart design, and can be used almost instantaneously at the start of process monitoring. The proposed control charts do not require any model fitting, thus, eliminating the problems associated with estimation errors, but might be used as part of a Phase-I study. Through a comprehensive performance comparison study under various out-of-control scenarios, the effectiveness of the charts in uncovering serial dependence is shown and recommendations for selection are given. Implementations of the proposed charts are illustrated by using batch yield data from a chemical process.

ARTICLE HISTORY

Received July 2022

Accepted December 2022

KEYWORDS


Nonlinear time series;
Nonparametric control
charts; Ordinal patterns;
Self-starting control charts;
Serial dependence

Dedicated to the memory of Karsten Keller (1961–2022).

1. Introduction

To monitor a stochastic process for possible deviations from its anticipated process model, the so-called in-control model, the most popular tool of statistical process control (SPC) is control charts. Control charts are a type of sequential hypothesis tests, where the null hypothesis is expressed in terms of the in-control model, and where the out-of-control models constitute the alternative hypothesis. Serial independence of observations is a crucial assumption for the majority of control charts used in SPC, see for example, Chakraborti and Sparks (2020). Either the monitored data themselves are assumed to be generated independently (Montgomery 2009), or if being concerned with time-series data, control charts are often applied to residuals computed from a model, where the residuals are uncorrelated if the in-control model is adequate for the process (Knoth and Schmid 2004). On the other hand, it is well known that if serial dependence is apparent and neglected, this may severely affect a control chart's performance (see the seminal studies by Alwan and Roberts (1988), Alwan (1992), Wardell, Moskowitz, and Plante (1992) and the more general discussion in Altioek and Melamed (2001)). Hence, it is of utmost importance to not only monitor a given process for possible changes in the mean or variance, but to also monitor for the in-control assumption of serial independence, to avoid a misleading chart performance.

There have been several contributions to the SPC literature during the last decades to monitor for existence of serial dependencies in real-valued and continuously distributed processes. The large majority of these contributions refer to the specific case of autoregressive moving-average (ARMA) time series models. Some of these directly incorporate the model structure into the monitored statistics, such as the cumulative sum (CUSUM) charts by Bagshaw and Johnson (1977), the sequential score tests by Hawkins (1984), the neural-network approach by Hwang (2005), the χ^2 -chart by Atienza and Tang (2006), or the CUSUM and Shiryaev–Roberts charts by Polunchenko and Raghavan (2018); the reader is also referred to Dooley and Kapoor (1990) for a more general discussion. Other studies are easier to generalize as they monitor the residuals (obtained with respect to an in-control model) for possible dependence, and are thus applicable to general serially independent processes as well. This approach is considered in the control charts proposed by Yourstone and Montgomery (1989, 1991) monitoring the residuals' autocorrelation function (ACF), their extension to an exponentially weighted moving-average (EWMA) chart by Atienza, Tang, and Ang (1997), the residuals' sum-of-square chart by Ermer, Chow, and Wu (1979), and the periodogram chart by Beneke et al. (1988). All these charts (as well as the aforementioned charts by Hwang 2005; Atienza and Tang 2006) rely on a moving-window approach, that is, successive and typically overlapping segments of some length w are drawn from the process and used for computing the involved

CONTACT Christian H. Weiß  weissc@hsu-hh.de  Department of Mathematics and Statistics, Helmut Schmidt University, 22043 Hamburg, Germany.

 Supplementary materials for this article are available online. Please go to www.tandfonline.com/r/TECH.

© 2023 The Author(s). Published with license by Taylor & Francis Group, LLC.

This is an Open Access article distributed under the terms of the Creative Commons Attribution-NonCommercial-NoDerivatives License (<http://creativecommons.org/licenses/by-nc-nd/4.0/>), which permits non-commercial re-use, distribution, and reproduction in any medium, provided the original work is properly cited, and is not altered, transformed, or built upon in any way.

statistics such as the ACF or periodogram. The typical window-length recommendation is $w = 50$, which leads to an important drawback such that w observations need to be collected before being able to compute the first statistic and therefore, an out-of-control situation can be detected with an initial delay of at least w observations. Control charts for monitoring individual residuals are also considered in the literature, for instance English et al. (2000) uses the ordinary EWMA chart to uncover changes in the dependence structure, and Gardner (1983) proposes an EWMA-type monitoring of the ACF at lag 1. Finally, although not a sequential procedure, a change-point test is also considered in Dürre and Fried (2020).

The control charts discussed so far exhibit at least one of the following drawbacks:

- they may be connected to a particular time-series model;
- distribution of the monitored statistic may depend on the actual type of the (residuals') marginal distribution (e.g., the assumption of normality is quite common in SPC, see Khakifirooz, Tercero-Gómez, and Woodall 2021);
- parameter estimation may be necessary for chart design (causing uncertainty with respect to the charts' true performance, see Jensen et al. 2006);
- they may react to out-of-control situations with a non-negligible initial delay caused by a moving-window approach.

In the following, we contribute to the literature on nonparametric control charts (see Chakraborti and Graham 2019; Koutras and Triantafyllou 2020 for recent surveys) by proposing new control charts that do not possess the aforementioned drawbacks. Proposed charts are; fully nonparametric and distribution-free, do not require any parameter estimation but have a unique chart design, can be used almost instantaneously at the start of process monitoring, and are applicable to any real-valued and continuously distributed process (which is assumed to be serially independent in its in-control state). Here, process monitoring does not only refer to the prospective monitoring during Phase II, the proposed charts might also be used as a tool for Phase-I analyses (Jones-Farmer et al. 2006). These appealing properties of the proposed charts are achieved by using so-called ordinal patterns for process monitoring, which are explained next in Section 2. Various control chart proposals for process monitoring are given in Section 3 and their designs are provided in Section 4. Then out-of-control performance of the proposed control charts are analyzed in Section 5 under diverse out-of-control scenarios. Finally, Section 6 illustrates the application of the proposed charts by using batch yields data from a chemical process and Section 7 concludes and outlines possible directions for future research.

2. Ordinal Patterns in Time Series

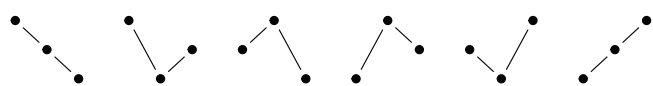
Since the seminal papers by Bandt and Pompe (2002) and Keller, Sinn, and Emonds (2007), ordinal patterns (OPs) have been widely used for analyzing real-valued time series (see, e.g., Bandt 2019 for recent references). Among others, they are used to check for serial dependence in such time series, see Caballero-Pintado et al. (2019), Bandt (2019), Weiß et al. (2022), Weiß (2022) for recent contributions. For a given real-valued

and continuously distributed process X_1, X_2, \dots , abbreviated as $(X_t)_{t \in \mathbb{N}}$ with $\mathbb{N} = \{1, 2, \dots\}$, the idea is to take a segment of some specified length $m \in \mathbb{N}$ with $m \geq 2$ at each time t , and to map this segment on its corresponding OP of order m (details are provided below). Based on the observed frequency of OPs, one judges the null hypothesis of serial independence for $(X_t)_{t \in \mathbb{N}}$. By contrast to the ACF, which is the default tool for dependence analyses, OP-statistics may also be sensitive to nonlinear forms of serial dependence.

Let S_m denote the symmetric group of order m , which consists of the $m!$ possible permutations of the integers $\{1, \dots, m\}$. The permutations $\pi \in S_m$ can be used in various equivalent ways to represent the $m!$ different OPs of a vector $\mathbf{x} = (x_1, \dots, x_m) \in \mathbb{R}^m$, see Berger et al. (2019). The probably most intuitive approach (and the one used here) is the *rank representation*, where the entries of $\pi = (r_1, \dots, r_m) \in S_m$ are interpreted as ranks, that is,

$$r_k < r_l \Leftrightarrow x_k < x_l \text{ or } (x_k = x_l \text{ and } k < l) \quad (1)$$

for all $k, l \in \{1, \dots, m\}$. As an example, if $m = 2$, only two OPs are possible, namely the downward pattern (2, 1) and the upward pattern (1, 2). For $m = 3$, by contrast, six OPs are possible, namely

$$(3, 2, 1) \quad (3, 1, 2) \quad (2, 3, 1) \quad (1, 3, 2) \quad (2, 1, 3) \quad (1, 2, 3)$$


$$(2) \quad (2)$$

In practice, $m = 3$ like in (2) is the most common choice for the order of OPs, see Bandt (2019). While $m = 2$ results in an oversimplification of the considered process, $m \geq 4$ leads to too many different patterns such that the respective OP-frequencies may become extremely small. Therefore, our focus is also on OPs of order $m = 3$ in this article.

Remark 2.1. The rank representation (1) of OPs uses two conditions to guarantee a unique definition of the OP π . Theoretically, a continuously distributed vector \mathbf{X} exhibits ties (i.e., equal entries $X_k = X_l$ for $k \neq l$) with probability zero, that is, we have the strict ordering " $X_k < X_l$ " in (1) almost surely. But due to the finite measurement accuracy in practice, we sometimes observe ties " $x_k = x_l$ " within the observations \mathbf{x} , which are accounted for by the second condition in (1). We assume, however, that such ties occur at most rarely, that is, the effect of ties on the OP-frequencies is negligible.

Let us return to the monitored process $(X_t)_{t \in \mathbb{N}}$. At each time t , we take a segment of length m from this process (called the " m -history") and map it onto its OP $\pi \in S_m$. Here, one does not need to take adjacent observations, but one may also allow for a time delay $d \in \mathbb{N}$ between them (e.g., in view of possible higher-order dependencies). That is, the t th m -history equals $\mathbf{X}_t^{(d)} = (X_t, X_{t+d}, \dots, X_{t+(m-1)d})$, and its OP is denoted by $\pi_t^{(d)}$. In this way, the original process $(X_t)_{t \in \mathbb{N}}$ is transformed into the OP-process $(\pi_t^{(d)})_{t \in \mathbb{N}}$. In the special case $d = 1$ (adjacent observations), we simply write \mathbf{X}_t and π_t instead of $\mathbf{X}_t^{(1)}$ and $\pi_t^{(1)}$, respectively. In fact, as $d = 1$ is most relevant in applications, we shall focus our later analyses on that case, but we provide the definition of our control charts for the case of general d . Note that

we define $\pi_t^{(d)}$ based on $X_t, X_{t+d}, \dots, X_{t+(m-1)d}$ for notational simplicity, as the resulting OP-process then uniquely starts at $t = 1$. But $\pi_t^{(d)}$ is finished only after having observed $X_{t+(m-1)d}$. Furthermore, successive OPs might overlap, in the sense that parts of the m -history coincide. For this reason, the OP process $(\pi_t^{(d)})_{\mathbb{N}}$ itself is not serially independent, see Weiß (2022) for further details. The consideration of all OPs, in turn, that is, at any time $t \in \mathbb{N}$, offers the opportunity of a timely detection of an out-of-control scenario, as always the full available information is used for process monitoring.

Example 2.2. To illustrate the computation of OPs, let us look at the first few observations from our data example in Section 6, which is about yields from a chemical process. To derive the OPs π_t with $m = 3$ and $d = 1$, we continually extract three subsequent observations $\mathbf{x}_t = (x_t, x_{t+1}, x_{t+2})$ for $t = 1, 2, \dots$, and determine their ranks (2) according to (1). Doing this, the data points

$$\begin{aligned} x_1 &= 47, & x_2 &= 64, & x_3 &= 23, & x_4 &= 71, \\ x_5 &= 38, & x_6 &= 64, & x_7 &= 55, & x_8 &= 41, \dots \end{aligned}$$

are transformed into

t	1	2	3	4	5	6
\mathbf{x}_t	(47, 64, 23)	(64, 23, 71)	(23, 71, 38)	(71, 38, 64)	(38, 64, 55)	(64, 55, 41)
π_t	(2, 3, 1)	(2, 1, 3)	(1, 3, 2)	(3, 1, 2)	(1, 3, 2)	(3, 2, 1)

The following two properties of the OP-process $(\pi_t^{(d)})_{\mathbb{N}}$ are crucial for the control charts proposed in the subsequent section:

1. OPs are invariant with respect to strictly monotonically increasing transformations of X_t . Thus, the (inverse) probability integral transform implies that OPs do not depend on the actual marginal distribution of $(X_t)_{\mathbb{N}}$, that is, OPs lead to a distribution-free approach.
2. If $(X_t)_{\mathbb{N}}$ is in its in-control state, it is assumed to be iid. Since the iid-property implies the exchangeability of the components in each m -history $\mathbf{X}_t^{(d)}$, it follows that $\pi_t^{(d)}$ has a discrete uniform distribution on S_m , that is, we have the probability mass function (PMF) $P(\pi_t^{(d)} = \pi) = 1/m!$ for each $\pi \in S_m$.

3. Control Charts based on Ordinal Patterns

Let $\pi^{[1]}, \dots, \pi^{[m]}$ denote the different m th-order OPs (i.e., the elements of S_m) in some arrangement (“lexicographic order”). We abbreviate the marginal probabilities of the OP-process by $p_k^{(d)} = P(\pi_t^{(d)} = \pi^{[k]})$ and define the $m!$ -dimensional PMF vector $\mathbf{p}^{(d)} = (\dots, p_k^{(d)}, \dots)$. If the process $(X_t)_{\mathbb{N}}$ is iid (in-control assumption), then all probabilities $p_k^{(d)}$, $k = 1, \dots, m!$, are equal to $1/m!$; let us abbreviate $\mathbf{p}_0 = (1/m!, \dots, 1/m!)$. This property is later used when designing the proposed control charts. The purpose of these control charts is to detect the presence of serial dependence (as soon as possible), which defines the possible out-of-control scenarios.

Several OP-statistics have been discussed in the literature that might be used to analyze the serial dependence structure of $(X_t)_{\mathbb{N}}$. Probably the most well-known statistic is the

permutation entropy dating back to Bandt and Pompe (2002), which is defined as $H^{(d)} = -\sum_{k=1}^{m!} p_k^{(d)} \ln p_k^{(d)}$. Under in-control conditions, $\mathbf{p}^{(d)}$ equals the uniform distribution \mathbf{p}_0 , and the permutation entropy $H^{(d)}$ equals $\ln m!$. If $\hat{\mathbf{p}}^{(d)}$ denotes an estimator of $\mathbf{p}^{(d)}$ and is plugged into the formula for $H^{(d)}$, then we denote resulting sample permutation entropy by $\hat{H}^{(d)}$, and the subsequent H -chart compares the t th value of $\hat{H}^{(d)}$ to the in-control value $\ln m!$.

As a possible modification of $H^{(d)}$, Weiß (2022) suggested to consider the permutation entropy $H_{\text{ex}}^{(d)} = -\sum_{k=1}^{m!} (1 - p_k^{(d)}) \ln(1 - p_k^{(d)})$ instead, which takes the value $(m! - 1) \ln(m!/(m! - 1))$ under in-control conditions. A further alternative is the distance to white noise (see Bandt 2019), which is defined as $\Delta^{(d)} = \sum_{k=1}^{m!} (p_k^{(d)} - 1/m!)^2$ and equals zero under in-control conditions. Let us summarize the sample versions of these entropy-type statistics in the following equation:

$$\begin{aligned} \hat{H}^{(d)} &= -\sum_{k=1}^{m!} \hat{p}_k^{(d)} \ln \hat{p}_k^{(d)}, \\ \hat{H}_{\text{ex}}^{(d)} &= -\sum_{k=1}^{m!} (1 - \hat{p}_k^{(d)}) \ln(1 - \hat{p}_k^{(d)}), \\ \hat{\Delta}^{(d)} &= \sum_{k=1}^{m!} (\hat{p}_k^{(d)} - 1/m!)^2. \end{aligned} \quad (3)$$

In Weiß (2022), it was shown that all these entropy-type OP-statistics are *asymptotically* equivalent, being related to the same asymptotic quadratic-form distribution. But if used as a hypothesis test for the null hypothesis of serial independence, they slightly differ in their finite-sample properties (often with a slight advantage for $\hat{H}_{\text{ex}}^{(d)}$). Note that a further modification, the so-called “symbolic correlation integral,” has also been proposed by Caballero-Pintado et al. (2019), however, as this is equivalent to $\hat{\Delta}^{(d)}$ (except a linear transformation), it is not further considered here.

The entropy-type OP-statistics (3) are well defined for any $m \geq 2$. For the particular case $m = 3$, which we focus on here, Bandt (2019) proposed a couple of further statistics, which are linear expressions in $\hat{\mathbf{p}}^{(d)}$:

$$\begin{aligned} \text{up-down balance: } \hat{\beta}^{(d)} &= \hat{p}_6^{(d)} - \hat{p}_1^{(d)}, \\ \text{persistence: } \hat{\tau}^{(d)} &= \hat{p}_6^{(d)} + \hat{p}_1^{(d)} - \frac{1}{3}, \\ \text{up-down scaling: } \hat{\delta}^{(d)} &= \hat{p}_4^{(d)} + \hat{p}_5^{(d)} - \hat{p}_3^{(d)} - \hat{p}_2^{(d)}. \end{aligned} \quad (4)$$

Bandt (2019) also discussed a fourth type of linear statistic, referred to as the “rotational asymmetry.” Nevertheless, in the simulation study on hypothesis tests by Weiß (2022), the rotational asymmetry showed a poor performance in any considered power scenario and thus, it is not further considered here.

Using statistics (3) and (4), we now define six types of control charts based on OPs. The basic idea is to use an EWMA approach, that is, exponential smoothing, for updating the OPs’ PMF vector $\hat{\mathbf{p}}_t^{(d)}$ computed from the OPs $\pi_1^{(d)}, \dots, \pi_t^{(d)}$ being available up to time t . This is done by using the $m!$ -dimensional binary vectors $\mathbf{Z}_t^{(d)}$, which are defined by the “one-hot encoding” $Z_{t,k}^{(d)} = \mathbb{1}(\pi_t^{(d)} = \pi^{[k]})$. Here, the indicator function $\mathbb{1}(A)$ equals 1 (0) if A is true (false). Note that $E[\mathbf{Z}_t^{(d)}] = \mathbf{p}_0$ under in-control conditions. For a given smoothing parameter $\lambda \in (0; 1)$, we define

$$\hat{\mathbf{p}}_0^{(d)} = \mathbf{p}_0, \quad \hat{\mathbf{p}}_t^{(d)} = \lambda \mathbf{Z}_t^{(d)} + (1 - \lambda) \hat{\mathbf{p}}_{t-1}^{(d)} \quad \text{for } t = 1, 2, \dots \quad (5)$$

Note that the elements of the vectors $\hat{\mathbf{p}}_t^{(d)}$ in (5) sum up to one. An EWMA approach like in (5) has been used for the monitoring of categorical time series by several authors, such as Ye et al. (2002), Weiß (2008), and Li, Tsung, and Zou (2014); Wang, Su, and Xie (2018).

As the last step to get control charts based on (3)–(5), appropriate control limits (CLs) have to be defined. Here, as usual, a control chart triggers an alarm once its control limits are violated. The time until the first alarm is referred to as the run length of the chart, which should be large (short) if the process is in control (out of control). Abbreviate the lower (upper) control limit by LCL (UCL). We now define the following one- or two-sided control charts by plugging-in $\hat{\mathbf{p}}_t^{(d)}$ into (3) and (4):

- H -chart: plot $\hat{H}_t^{(d)}$ with LCL $l_H \in (0; \ln m!)$;
- H_{ex} -chart: plot $\hat{H}_{\text{ex},t}^{(d)}$ with LCL $l_{H_{\text{ex}}} \in (0; (m! - 1) \ln(\frac{m!}{m!-1}))$;
- Δ -chart: plot $\hat{\Delta}_t^{(d)}$ with UCL $l_{\Delta} > 0$;
- β -chart: plot $\hat{\beta}_t^{(d)}$ with UCL $l_{\beta} > 0$ and LCL $-l_{\beta}$;
- τ -chart: plot $\hat{\tau}_t^{(d)}$ with UCL $l_{\tau} > 0$ and LCL $-l_{\tau}$;
- δ -chart: plot $\hat{\delta}_t^{(d)}$ with UCL $l_{\delta} > 0$ and LCL $-l_{\delta}$.

The “linear charts” β , τ , and δ have symmetric two-sided control limits, because their in-control distribution is symmetric with mean 0. The entropy-type charts H , H_{ex} , and Δ in (6) are one-sided charts with baselines $\ln m!$, $(m! - 1) \ln(\frac{m!}{m!-1})$, and 0, respectively. If the user prefers not to use the lower-sided design of the H - and H_{ex} -chart, one can equivalently monitor $\ln m! - \hat{H}_t^{(d)}$ and $(m! - 1) \ln(\frac{m!}{m!-1}) - \hat{H}_{\text{ex},t}^{(d)}$ with baselines 0 and UCLs $\ln m! - l_H$ and $(m! - 1) \ln(\frac{m!}{m!-1}) - l_{H_{\text{ex}}}$, respectively.

Remark 3.1. There is a relation between the monitoring of OPs and the use of so-called “sensitizing rules” for Shewhart control charts, see Sections 5.3.5–6 in Montgomery (2009) for an overview. Some of these rules may indicate a “nonrandom pattern of behavior”, that is, a violation of the independence assumption (the most common rules are summarized in Table 5.1 (p. 197) of Montgomery (2009)). Among them, especially rules 5 and 7 are related to the OPs in (2) with $m = 3$ and $d = 1$:

- “5. Six points in a row steadily increasing or decreasing.”
This rule can be expressed in terms of either the strictly decreasing OP $\pi^{[1]} = (3, 2, 1)$ or strictly increasing OP $\pi^{[6]} = (1, 2, 3)$ from (2): one of these OPs must occur four times in immediate succession.
- “7. Fourteen points in a row alternating up and down.”
Here, we consider the group $\{\pi^{[2]}, \pi^{[5]}\} = \{(3, 1, 2), (2, 1, 3)\}$ of “down-up” OPs, and $\{\pi^{[3]}, \pi^{[4]}\} = \{(2, 3, 1), (1, 3, 2)\}$ of “up-down” OPs. Rule 7 corresponds to an OP-sequence of length 12 in which the patterns from both groups alternate in their appearance.

Also note that the OPs being relevant for rule 5 are considered by the β - and τ -statistic in (4), whereas the OPs for rule 7 are used for the δ -statistic.

Generally, the aforementioned sensitizing rules correspond to the repeated occurrence of some specific OPs. This, however, also affects the EWMA statistic $\hat{\mathbf{p}}_t = \hat{\mathbf{p}}_t^{(1)}$ in (5). For example, if $\pi^{[1]}$ occurs four times in immediate succession, say at times $t + 1, \dots, t + 4$, then $\hat{\mathbf{p}}_{t+4,1}$ increases according to

$$\begin{aligned}\hat{p}_{t+4,1} &= \lambda + \lambda(1 - \lambda) + \lambda(1 - \lambda)^2 + \lambda(1 - \lambda)^3 + (1 - \lambda)^4 \hat{p}_{t,1} \\ &= 1 - (1 - \lambda)^4 + (1 - \lambda)^4 \hat{p}_{t,1},\end{aligned}$$

whereas the remaining probabilities decrease as $\hat{p}_{t+4,i} = (1 - \lambda)^4 \hat{p}_{t,i}$ for $i \neq 1$. This may cause an alarm by some of the charts in (6), for example, the β -chart. However, the OP-charts are not limited to the few types of “nonrandom patterns” expressed by rules 5 and 7, but they provide a much broader view on the monitored process. This is also important in view of the fact that these rules are not particularly effective in some cases, see, for example, the study by Davis and Woodall (1988).

To sum up, as no distributional assumptions are required for $(X_t)_{\mathbb{N}}$ except that X_t is continuously distributed, the proposed OP-based control charts are fully nonparametric. Since the distribution for $\pi_t^{(d)}$ is uniform and always the same under in-control process conditions, model estimation is not required and this avoids effects of estimation uncertainty on the OP-charts’ performance. Thus, while the chart design does not need a preceding Phase-I analysis, the proposed OP-charts could be applied also during Phase I to check if the in-control assumption of serial independence is justified. In a sense, these charts can also be classified as self-starting, where we update the available information on the true OP-distribution by using the EWMA approach. The first statistic being plotted on the chart relies on $\pi_1^{(d)}$, and this is available with observation $X_{1+(m-1)d}$, that is, with an initial delay of $(m-1)d$. This delay, however, is negligible in practice as $m = 3$ and $d = 1$ are the most common choices, that is, control charting starts after having observed X_1, X_2, X_3 .

4. Design of OP-Charts

Although some asymptotic results are provided by Weiß (2022), the exact distribution of the OP-statistics in (3) and (4) is not known. Furthermore, while the marginal distribution of the OP-process $(\pi_t^{(d)})_{\mathbb{N}}$ under in-control conditions is a simple uniform distribution, the OP-process itself is not iid but exhibits MA($m - 1$)-dependence, which is superimposed by the dependence caused by the EWMA approach (5). Consequently, an exact computation of the run-length distribution of the EWMA charts in (6), and especially of their average run length (ARL, i.e., the average time until the first alarm), is not possible. Thus, ARLs have to be approximated based on simulations, see the details below. On the other hand, a highly attractive feature of the control charts in (6) for the user is the fact that the in-control design for each setting (m, d, λ) and for each target ARL value (denoted as ARL_0) needs to be determined only once, independent of the actual marginal distribution of $(X_t)_{\mathbb{N}}$ and without model estimation, as OPs are distribution-free. Our simulation-based chart design used 10^5 replications for each ARL computation throughout the article. For a given setting (m, d, λ) , and for a fixed choice of the CLs, the process $(X_t)_{\mathbb{N}}$ is generated under in-control conditions in each simulation run,

Table 1. In-control design (CLs) of EWMA OP-charts (6) with $m = 3, d = 1$, and target $ARL_0 \approx 370$; different smoothing parameters λ .

λ	H -chart		H_{ex} -chart		Δ -chart		β -chart		τ -chart		δ -chart	
	I_H	ARL	$I_{H_{ex}}$	ARL	I_Δ	ARL	I_β	ARL	I_τ	ARL	I_δ	ARL
0.25	1.014	367.8	0.6621	369.6	0.3338	369.3	0.6437	369.7	0.4253	368.6	0.7656	368.4
0.10	1.4601	369.8	0.8405	369.9	0.1115	369.5	0.3638	369.9	0.2529	369.8	0.4876	370.4
0.05	1.6356	370.0	0.88017	369.3	0.05125	370.3	0.233	370.0	0.16775	369.4	0.3246	369.5

NOTE: Designs applicable to any continuously-distributed process (without necessity of model estimation).

and the time until the first alarm (run length) is determined. Taking the mean across all 10^5 simulated run lengths, we get an approximate value for the in-control ARL for the considered setting (m, d, λ) and CLs. For chart design given (m, d, λ) , this procedure is iteratively repeated for varying values of the CLs (taken from a specified grid of values), and we decide for those CLs that lead to an in-control ARL closest to the given target ARL_0 .

In what follows, we focus on OPs of order $m = 3$, delay $d = 1$, and $ARL_0 \approx 370$ as this is a common textbook choice (Montgomery 2009). More precisely, the in-control design is based on the so-called “zero-state ARL” (Knoth 2006), while possible alternative ARL concepts are briefly discussed in Section 5, where the charts’ out-of-control performance is analyzed. Certainly, because of the discreteness of the OPs $(\pi_t)_{\mathbb{N}}$, this target ARL_0 can usually not be met exactly, so the designs were chosen (by a grid search) to ensure an in-control ARL close to ARL_0 . Furthermore, we considered different choices of the smoothing parameter λ , namely $\lambda \in \{0.25, 0.10, 0.05\}$. Having done these specifications, simulations for chart design can be done with an arbitrary marginal distribution for the iid in-control process $(X_t)_{\mathbb{N}}$. We used iid standard-normal variates for simplicity, but any other continuous distribution would have led to the same result. In other words, the obtained chart designs in Table 1 are valid for any continuously-distributed iid process (independent of its actual parameterization and without the need for parameter estimation) and might thus be directly used by the reader.

Regarding the designs in Table 1, it can be seen that the control limits get narrower if λ decreases, which is reasonable as decreasing λ intensifies the effect of smoothing. For the same reason, one generally gets closer to the target ARL_0 if λ is small, whereas the effects of discreteness are more pronounced for larger values of λ such as $\lambda = 0.25$. In the next Section 5, the chart designs in Table 1 are used for a simulation study, where the out-of-control ARL performance of the charts is analyzed.

5. Performance Analyses of OP-Charts

The control charts of Table 1 are now analyzed with respect to their out-of-control performance, where diverse types of out-of-control scenarios are considered. Throughout this section, we omit replicating the in-control ARLs from the Table 1, as these are sufficiently close to the target $ARL_0 \approx 370$ such that a fair comparison is ensured. Our simulation study covers both linear and nonlinear data-generating processes (DGPs), all having an AR-structure with dependence parameter α , where $\alpha = 0$ corresponds to the in-control assumption of iid data. In the following list of DGPs, $N(\mu, \sigma^2)$ denotes the normal distribution with mean $\mu \in \mathbb{R}$ and variance $\sigma^2 > 0$, and $\text{Exp}(1/\mu)$ is the exponential distribution with mean $\mu > 0$:

DGP 1: AR(1) process $X_t = \alpha \cdot X_{t-1} + \epsilon_t$ with $\epsilon_t \sim N(0, 1)$;

DGP 2: TEAR(1) (transposed exponential AR) process $X_t = B_t^{(\alpha)} \cdot X_{t-1} + (1 - \alpha) \cdot \epsilon_t$ with $\epsilon_t \sim \text{Exp}(1)$, where the iid Bernoulli random variables $B_t^{(\alpha)}$ with $P(B_t^{(\alpha)} = 1) = \alpha$ are generated independently of $(\epsilon_t)_{\mathbb{Z}}$ and $(X_s)_{s < t}$;

DGP 3: AAR(1) (absolute AR) process $X_t = \alpha \cdot |X_{t-1}| + \epsilon_t$ with $\epsilon_t \sim N(0, 1)$;

DGP 4: QAR(1) (quadratic AR) process $X_t = \alpha \cdot X_{t-1}^2 + \epsilon_t$ with $\epsilon_t \sim N(0, 1)$.

For all of these DGPs, innovations $(\epsilon_t)_{\mathbb{Z}}$ are iid so that we have exponential white noise (with mean 1) for DGP 2, and Gaussian white noise otherwise. DGP 1 is a linear (and time-reversible) process, which is described in any textbook on time series analysis, such as Box and Jenkins (1970). By contrast to the remaining DGPs, the dependence parameter α is also allowed to take negative values, that is, it can also be used to generate negative autocorrelation. The DGPs 3 and 4 are nonlinear modifications of DGP 1, where $|X_{t-1}|$ or X_{t-1}^2 , respectively, cause positive shocks (and thus asymmetry) to the process. The DGP 4, proposed by Lawrance and Lewis (1981), has an exponentially decaying ACF like DGP 1, namely $\rho(h) = \text{corr}[X_t, X_{t-h}] = \alpha^h$, but lacks time reversibility (i.e., joint distributions may be asymmetric in time). For the DGPs 1 and 2, the stationary marginal distribution is known, namely $N(0, \frac{1}{1-\alpha^2})$ and $\text{Exp}(1)$, whereas it is unknown and nonstandard for the DGPs 3 and 4. As a consequence, when simulating stationary processes, a prerun for burn-in is required for the DGPs 3 and 4, where we used the prerun length of 100.

Tables 2–5 summarize the zero-state out-of-control ARLs obtained for the DGPs 1–4. As detailed in Knoth (2006), a zero-state ARL is computed under the premise that the process is out-of-control right from the beginning of process monitoring (i.e., the change point $\tau = 1$). There are also other ARL concepts, where the process change happens later (i.e., a change point $\tau > 1$). For details, please see the discussion in Remark 5.1. However, as zero-state ARLs are most common in the SPC literature, our main focus is on zero-state ARLs here. Furthermore, we demonstrate in Remark 5.1 that for the considered OP-charts, the difference between different ARL concepts is negligible (while this difference has been shown to be large for some other control charts, see Knoth et al. (2021)). Table 2 provides the ARLs for the case of the linearly dependent AR(1) process. Here, we omitted the β - and δ -chart since it was already shown in Weiß (2022) that these statistics are not sensitive to linear dependence. The left part of Table 2 shows the ARLs with respect to positive dependence where decreasing ARLs for increasing α can be seen throughout. The best performance is observed for the τ -chart and it is interesting to see that the ARL performance gets slightly worse if λ is smaller than 0.25. The same pattern with respect to λ (even more pronounced) is also observed for the

Table 2. Out-of-control ARLs under DGP 1 of relevant EWMA OP-charts (6) with designs from Table 1.

α	H	H_{ex}	Δ	τ	α	H	H_{ex}	Δ	τ
$\lambda = 0.25$									
0.2	231.9	217.8	217.6	185.4	-0.2	588.0	647.8	640.2	798.2
0.4	143.7	128.0	128.5	101.8	-0.4	942.4	1174.4	1162.0	1840.3
0.6	85.9	75.2	75.3	60.4	-0.6	1255.2	2324.6	2266.1	4634.4
0.8	50.6	44.7	44.8	39.2	-0.8	491.8	5508.4	5242.5	13649.7
$\lambda = 0.10$									
0.2	299.8	233.7	242.2	191.3	-0.2	411.1	570.5	531.3	411.2
0.4	212.4	145.1	152.9	99.9	-0.4	392.8	786.8	681.8	203.7
0.6	135.3	89.3	94.2	59.7	-0.6	242.3	692.3	565.1	83.8
0.8	81.7	54.7	57.6	40.5	-0.8	85.7	231.6	190.8	37.4
$\lambda = 0.05$									
0.2	303.3	261.2	269.5	206.2	-0.2	349.0	424.2	411.2	271.4
0.4	208.3	166.2	172.9	105.7	-0.4	237.8	347.7	326.2	118.0
0.6	132.4	104.0	108.7	63.8	-0.6	120.6	180.6	168.2	56.2
0.8	84.5	67.2	69.4	43.9	-0.8	57.0	75.1	71.3	30.7

remaining charts. For negative dependence in the right part of Table 2, by contrast, we observe the opposite phenomenon. For $\lambda = 0.25$, none of the charts should be used as the out-of-control ARLs even exceed ARL_0 (i.e., the charts would be slower on average in detecting negative dependence than in triggering a false alarm under in-control conditions). For $\lambda = 0.10$, we still have a somewhat biased ARL performance (especially for H_{ex} - and Δ -chart), whereas for $\lambda = 0.05$, at least the H - and, in particular, the τ -chart perform quite well. Overall, the τ -chart with $\lambda = 0.05$ appears to be a good compromise, being sensitive to both positive and negative dependence. If only positive linear dependence is to be expected under out-of-control conditions, then the τ -chart is better equipped with $\lambda = 0.25$.

Let us now turn to nonlinear DGPs. While the DGP 2 still has the same ACF as DGP 1 (but restricted to only positive α), it is highly asymmetric in its temporal behavior. It tends to generate long-lasting rises, which are followed by abrupt falls. As a consequence, the strictly upward pattern (1, 2, 3) in (2) is observed exceptionally often. It is thus not surprising that the β -chart is superior in Table 3, because the β -statistic according to (4) directly compares the probabilities for the two strictly monotone OPs. However, also H -, H_{ex} -, and Δ -chart perform nearly equally well, where the ARL-performance also slightly improves with decreasing λ . The τ -chart now does visibly worse, but it is still much better than the δ -chart. In fact, the δ -chart did even worse for the other DGPs, so we do not recommend its use and omit its further discussion.

The remaining DGPs 3–4 are nonlinear modifications of DGP 1. The results for DGP 3 in Table 4 and for DGP 4 in Table 5 indicate that the preference for one of the charts depends on the anticipated out-of-control behavior. If low values of α are to be expected (say $\alpha \leq 0.4$ for DGP 3, or $\alpha \leq 0.2$ for DGP 4), the use of the β -chart with $\lambda = 0.05$ is recommended, but also H_{ex} - and Δ -chart do quite well. For larger α , by contrast, the τ -chart with $\lambda = 0.25$ is superior, but H_{ex} - and Δ -charts are again reasonable alternatives, especially for the DGP 4.

As an interim balance from Tables 2–5, the use of an appropriately chosen EWMA τ -chart appears to be a reasonable universal choice. Although not always the optimal chart, it never really fails, provided that λ is chosen adequately. If one has more information about the out-of-control scenario to be expected, a

Table 3. Out-of-control ARLs under DGP 2 of EWMA OP-charts (6) with designs from Table 1.

α	H	H_{ex}	Δ	β	τ	δ
$\lambda = 0.25$						
0.1	254.1	252.7	252.0	254.6	265.8	360.7
0.2	133.1	135.9	135.3	133.7	166.5	331.7
0.3	69.4	71.3	70.9	69.1	96.3	294.0
0.4	38.7	39.9	39.8	38.5	55.8	268.1
0.5	23.5	24.2	24.1	23.4	33.0	260.5
0.6	15.2	15.6	15.6	15.3	20.5	286.9
$\lambda = 0.10$						
0.1	254.1	236.2	238.4	231.1	286.0	337.6
0.2	126.9	114.0	115.5	108.8	191.0	255.8
0.3	65.8	58.5	59.2	55.1	113.6	183.6
0.4	38.5	33.9	34.4	32.0	65.1	140.0
0.5	24.9	21.7	22.1	20.6	38.3	115.5
0.6	17.4	15.1	15.3	14.5	23.6	110.8
$\lambda = 0.05$						
0.1	239.5	228.6	230.4	214.4	310.7	310.6
0.2	114.6	106.5	107.7	95.7	213.7	203.2
0.3	61.7	56.5	57.3	50.6	126.9	132.1
0.4	38.2	34.6	35.1	30.9	72.5	94.8
0.5	26.2	23.5	23.9	21.2	43.3	74.8
0.6	19.3	17.1	17.4	15.5	27.1	66.6

Table 4. Out-of-control ARLs under DGP 3 of relevant EWMA OP-charts (6) with designs from Table 1.

α	H	H_{ex}	Δ	β	τ
$\lambda = 0.25$					
0.2	329.4	330.0	329.6	334.0	326.6
0.4	242.6	238.2	237.8	252.9	229.0
0.6	157.6	146.8	147.0	169.9	132.0
0.8	89.3	79.1	79.3	101.7	68.1
$\lambda = 0.10$					
0.2	331.4	322.5	322.7	323.0	334.3
0.4	260.8	228.8	233.2	238.1	242.5
0.6	193.7	148.6	154.0	170.2	138.2
0.8	129.7	88.9	93.5	123.5	70.7
$\lambda = 0.05$					
0.2	326.0	319.3	320.5	313.1	346.5
0.4	250.3	230.3	234.1	224.7	264.3
0.6	184.2	156.3	160.7	164.9	150.4
0.8	126.7	100.9	104.7	136.6	76.0

Table 5. Out-of-control ARLs under DGP 4 of relevant EWMA OP-charts (6) with designs from Table 1.

α	H	H_{ex}	Δ	β	τ
$\lambda = 0.25$					
0.15	283.5	284.8	283.8	290.3	285.1
0.2	221.9	219.9	219.3	230.5	217.2
0.25	118.9	116.1	116.0	123.8	114.9
0.3	36.6	35.7	35.7	37.6	35.5
$\lambda = 0.10$					
0.15	289.6	271.8	273.6	271.7	302.8
0.2	237.0	211.3	214.7	215.1	234.0
0.25	131.4	114.5	116.6	118.6	122.3
0.3	40.8	36.8	37.3	37.9	37.7
$\lambda = 0.05$					
0.15	278.0	266.6	268.8	254.3	321.9
0.2	227.0	210.8	213.6	200.4	257.8
0.25	128.9	118.2	120.0	113.6	134.3
0.3	41.8	39.0	39.5	38.3	40.7

refined choice of the control chart can be done, such as H_{ex} - and Δ -chart for nonlinear processes in general or the β -chart for a TEAR(1) process (DGP 2) in particular.

Remark 5.1. As explained earlier in this section, our focus was on the zero-state ARL up to now, but other ARL concepts exist in the literature (see Knoth 2006). In particular, types of conditional expected delay (CED) are relevant for practice, as they do not assume the process to be out-of-control right from beginning (as the zero-state ARL does), but first allow for a certain in-control phase. More precisely, the CED with change point $\tau > 1$ assumes that the first $\tau - 1$ observations are generated under in-control conditions and that the chart does not trigger a false alarm during this period, but then turns to out-of-control with the τ th observation. Then, the CED is defined as the mean number of out-of-control observations until the first alarm, where the limit $\tau \rightarrow \infty$ leads to the so-called “steady-state ARL.” In our case, the first $\tau - 1$ observations are iid with the same marginal distribution as the out-of-control DGP, which we switch to for $t \geq \tau$. In Table 6, we see CEDs for $\tau = 101$, that is, the process was in-control for the first 100 observations. As the marginal distribution is only known for DGPs 1 and 2, we restrict ourselves to these DGPs, and results are shown for the smoothing parameter $\lambda = 0.1$.

Comparing the upper part of Table 6 to Table 2, and the lower part to Table 3, we recognize only small numerical differences between both types of ARL. We judge these differences as negligible for practice, not only because of their small numerical amounts, but also because they do not affect the ranking between the charts. This confirms that for the considered control charts, it does not make a difference if being faced with early or late process changes and, thus, an evaluation based on the zero-state ARL is sufficient.

To conclude the performance analyses of Section 5, let us look for possible competitors to monitor the dependence structure. As outlined in the literature review of Section 1, the large majority of dependence charts proposed so far make use of a moving window such that the first alarm is unavoidably delayed by the window length w (a common choice is $w = 50$). This would not be a problem if we expect only late process changes (and thus evaluate the performance based on the steady-state ARL). However, since a common aim of dependence monitoring is the detection of a misspecified in-control model (namely uncovering the erroneous assumption of serial independence, also see Section 6), it seems relevant that control charts for monitoring dependence also show a good performance regarding early process changes. For the OP-charts, we recognized a balanced ARL performance regarding both early and late changes, recall Remark 5.1.

Focusing on control charts, where the actual position of the change point is not relevant, only the EWMA-type control chart based on the lag-1 ACF, as it was proposed by Gardner (1983), seems to be a reasonable competitor, since it can also be used right from the start of process monitoring. This chart is designed based on simulations again, but now the chart design depends on the actual in-control model. As an illustrative example, we consider the in-control model of Gaussian white noise, that is, the X_t are iid $N(0, 1)$. Then, the statistics A_t , $t = 1, 2, \dots$, are defined by

$$\left. \begin{aligned} C_0 &= 0, & C_t &= \vartheta X_t X_{t+1} + (1 - \vartheta) C_{t-1}, \\ S_0 &= 1, & S_t &= \vartheta X_t^2 + (1 - \vartheta) S_{t-1}, \end{aligned} \right\} \Rightarrow A_t = \frac{C_t}{S_t}, \quad (7)$$

Table 6. Out-of-control CEDs ($\tau = 101$) under DGP 1 (upper part, to be compared to Table 2) and DGP 2 (lower part, to be compared to Table 3) of relevant EWMA OP-charts (6) with designs from Table 1 for $\lambda = 0.10$.

DGP 1									
α	H	H_{ex}	Δ	τ	α	H	H_{ex}	Δ	τ
0.2	289.6	227.5	236.3	185.6	−0.2	400.4	555.8	517.3	403.9
0.4	202.9	140.1	148.0	97.4	−0.4	379.7	771.7	668.6	196.7
0.6	129.9	86.9	91.2	59.0	−0.6	233.4	678.2	554.6	81.3
0.8	77.8	53.5	55.9	39.5	−0.8	82.9	227.5	186.3	36.7

DGP 2						
α	H	H_{ex}	Δ	β	τ	δ
0.1	247.1	230.8	232.9	227.4	282.1	329.6
0.2	122.3	110.5	111.7	105.7	186.2	250.4
0.3	63.4	56.9	57.5	54.1	111.0	180.7
0.4	36.9	33.0	33.3	31.3	63.8	136.2
0.5	23.9	21.3	21.5	20.6	37.9	113.7
0.6	16.8	14.9	15.1	14.5	23.6	107.9

Table 7. Out-of-control ARLs under DGP 1 (left part, to be compared to Table 2) and DGP 2 (right part, to be compared to Table 3) of EWMA ACF-chart (7); in-control model: iid $N(0, 1)$.

DGP 1						DGP 2		
α	$\vartheta = 0.25$	$\vartheta = 0.10$	α	$\vartheta = 0.25$	$\vartheta = 0.10$	α	$\vartheta = 0.25$	$\vartheta = 0.10$
0.2	271.8	137.8	−0.2	272.1	137.8	0.1	333.6	240.2
0.4	141.0	46.5	−0.4	142.1	46.7	0.2	291.3	149.4
0.6	71.2	24.1	−0.6	71.8	24.2	0.3	247.9	97.2
0.8	40.0	16.7	−0.8	40.0	16.7	0.4	210.6	66.8
						0.5	179.2	48.6
						0.6	154.0	36.5

where $\vartheta \in (0, 1)$, and they are plotted on a chart with symmetric CLs. For the specified in-control model, we choose the CLs ∓ 1.142 if $\vartheta = 0.25$, and ∓ 0.6 if $\vartheta = 0.10$, both leading to an in-control ARL of ≈ 369.7 . Note that the levels of the smoothing parameter ϑ in (7) and λ in (5) are not directly comparable. As the OP-process is highly discrete (with only six possible outcomes), smaller smoothing parameters are required to dampen the effect of discreteness.

Before doing simulations, the out-of-control scenarios have to be adapted as the ACF-chart depends on the parametric $N(0, 1)$ -assumption. For the DGP 1, we use $\epsilon_t \sim N(0, 1 - \alpha^2)$ to ensure the $N(0, 1)$ -marginal. For the DGP 2, we transform each observation X_t by applying $\Phi^{-1}(G(\cdot))$, where G and Φ denote the cumulative distribution functions of $\text{Exp}(1)$ and $N(0, 1)$, respectively. By this (inverse) probability integral transform, we change the TEAR(1)’s marginal distribution from $\text{Exp}(1)$ into $N(0, 1)$, such that chart (7) is applicable. For the DGPs 3 and 4, the marginal distribution is not known such that an appropriate chart design of (7) is not possible.

The ARLs of the ACF-chart in Table 7 uniquely improve if ϑ is reduced from 0.25 to 0.10. The ARLs for the DGP 1 (left part of Table 7), that is, the linear AR(1) process, have to be compared to Table 2. There, the recommended choice was the τ -chart with $\lambda = 0.05$, the out-of-control performance of which can be ranked between $\vartheta = 0.25$ and $\vartheta = 0.10$ for the ACF-chart. Generally, as the ACF is a measure of linear dependence, it is reasonable that the ACF-chart does quite well in uncovering AR(1) dependence. However, if faced with the nonlinear DGP 2 (right part of Table 7, to be compared to

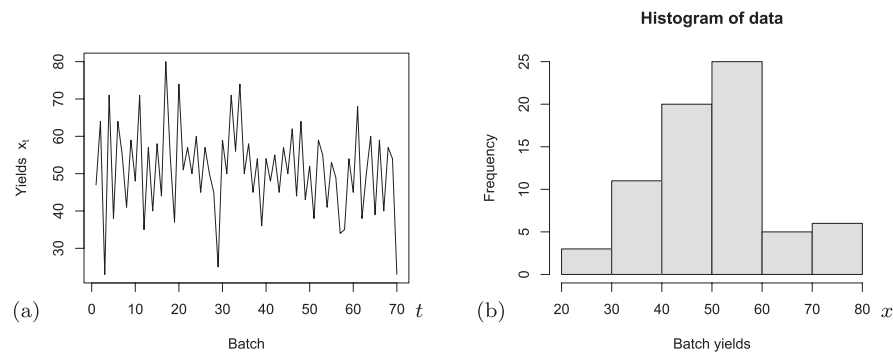


Figure 1. Chemical process data (x_t) of Section 6: (a) time series plot, and (b) histogram.

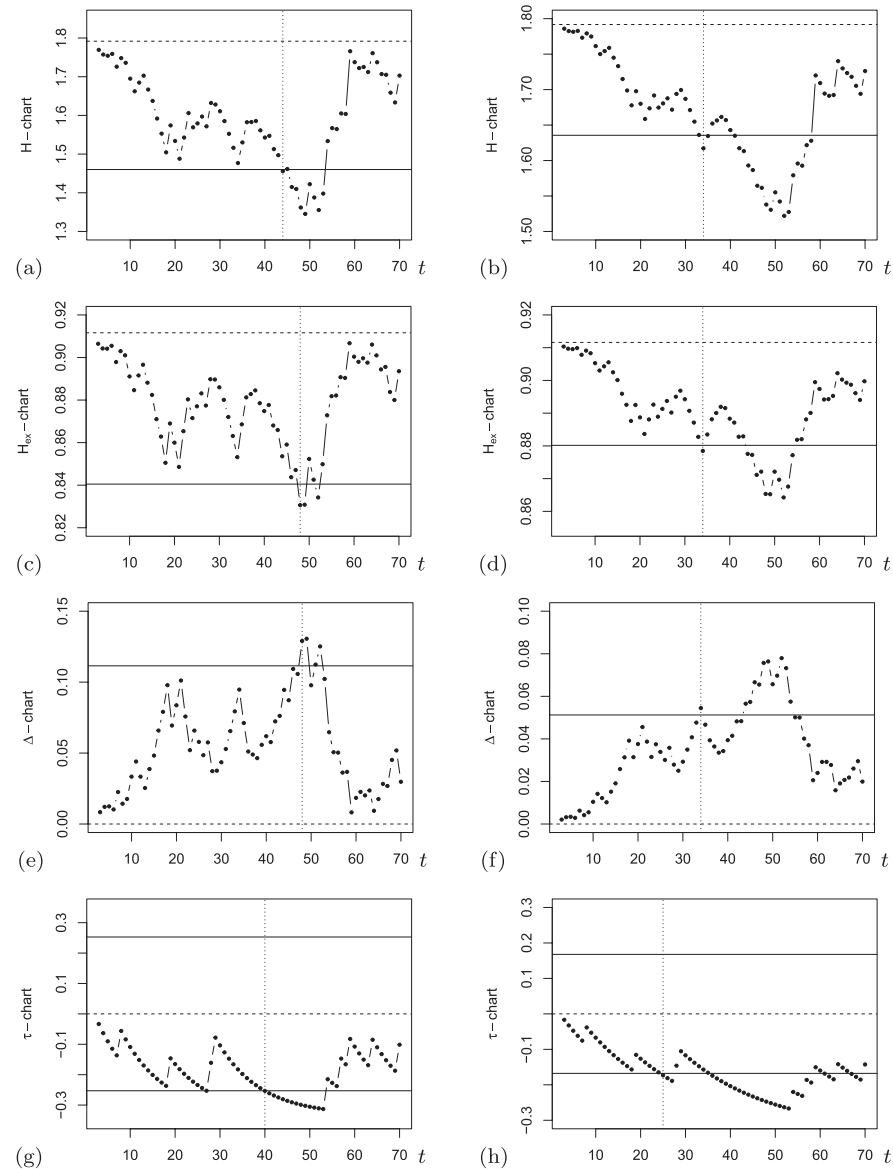


Figure 2. Chemical process data (x_t) of Section 6: H -, H_{ex} -, Δ -, and τ -charts for $\lambda = 0.10$ (left column) and $\lambda = 0.05$ (right column).

the Table 3), it does clearly worse than an appropriate OP-chart. For example, the H_{ex} -, Δ -, and β -charts with $\lambda \leq 0.1$ uniquely outperform any of the ACF-charts. Furthermore, the actual weakness of the ACF-chart is its parametric nature: a tailor-made chart design is necessary for any in-control model,

and the resulting ARL performance is also affected by estimation uncertainty. The distribution-free OP-charts, by contrast, have a universal chart design and, if appropriately chosen, they can recognize both linear and nonlinear dependence in an appealing way.

6. Illustrative Data Application

To illustrate the application of our OP-charts, let us pick up a well-known data example from the literature, namely the chemical process data x_1, \dots, x_{70} of Box and Jenkins (1970, Series F). These data consist of consecutive batch yields as shown in Figure 1(a). They have been analyzed, among others, by Beneke et al. (1988), who applied a periodogram chart for uncovering possible cyclic tendencies. Their chart design relies on the in-control assumption of iid Gaussian data. As this chart uses a moving window of length $w = 50$, it is impossible to get an alarm before having observed x_{50} . In fact, it takes until $t = 67$ for triggering the first alarm, indicating that the process is not iid.

Let us now apply appropriate OP-charts to these data. For this purpose, it is useful to think about plausible out-of-control scenarios. According to O'Donovan (1983, p. 34), it would be reasonable to observe negative dependence between adjacent batches, because residues caused by a high-yielding batch could reduce the yield of the subsequent batch (and vice versa). Therefore, in view of our findings in Section 5 (recall the discussion of Table 2), the H -, H_{ex} -, Δ -, and τ -charts constitute relevant candidates, where the smoothing parameter λ should be chosen small ($\lambda = 0.05$ led to the best ARL performance, with the τ -chart being superior). One of the major advantages of our OP-charts is given by the fact that we can apply them immediately to the data, by just using the designs from Table 1, but without the need for prior model fitting based on some Phase-I data. In fact, the histogram in Figure 1(b) indicates that it would be difficult to find an appropriate in-control model for these data. In particular, a normality assumption, such as it was used for chart design by Beneke et al. (1988), appears difficult to justify.

The obtained control charts are plotted in Figure 2 and their behavior nicely agrees with the theoretical ARL performances of Table 2. First, if using $\lambda = 0.25$ (not shown), none of the charts triggers an alarm, but the charts get more sensitive with decreasing λ . Second, for $\lambda = 0.10$ (left column), the first chart to trigger an alarm is the τ -chart (at observation $t = 40$), followed by the H -chart ($t = 44$), and followed by H_{ex} - and Δ -chart ($t = 48$). This is the same ranking as in Table 2. It is also worth noting that any of these charts is faster than the periodogram chart of Beneke et al. (1988). But the best results are indeed observed for $\lambda = 0.05$ (right column in Figure 2), where H -, H_{ex} -, and Δ -chart signal at $t = 34$, and the τ -chart even at $t = 25$, again in agreement to its superior ARL performance according to Table 2.

Hence, it seems clear that the in-control iid-assumption is violated. In fact, the lag-1 sample ACF of the full data, being ≈ -0.390 , is significantly negative, and the partial ACF is significant only at lag 1, that is, the data appear to be generated by a negatively dependent AR(1) process. The negative dependence also gets clear from Figure 1(a), where the data exhibit an alternating pattern. Nevertheless, despite these clear violations from iid, it would be difficult to reliably establish them based on the existing parametric control charts, because their chart design would require to first identify an appropriate in-control model for the data. Our distribution-free OP-charts, by contrast, are directly applicable, and they are quite powerful in uncovering serial dependence.

7. Conclusions

According to Chakraborti and Sparks (2020, p. 138), the two main limitations in applying control charts in practice are distributional assumptions (especially that of normality) and the assumption of serial dependence. Along with this, it is stated that *Violations of one or more of the assumptions might render the decisions invalid and hence useless even though there would seem nothing wrong in terms of crunching the numbers*. In this respect, we proposed control charts for monitoring serial dependence in the data. The proposed charts are highly attractive from an implementation point of view since they do not rely on distributional assumptions and corresponding model estimation, avoiding the first issue. Besides, it is shown that these charts can be useful in uncovering serial dependence in data and thus help to avoid the second issue. Furthermore, a Phase-I study for designing the proposed OP-charts is not needed, reducing the time to start implementation as well as the problems associated with errors in parameter estimation.

The proposed charts can be used when an iid model: (i) for the observations from the process or (ii) for the residuals of a time series model of the process, is appropriate for an in-control process but serial dependence is anticipated in the process observations or time series model residuals when the process is out of control. Designs for these charts are provided, which are applicable to any continuously distributed process without the necessity of model estimation. Using various performance comparison scenarios and illustration through the well-known batch yield data from the literature, it is shown that the proposed charts can be useful in monitoring for the existence of serial dependence. Among the proposed charts, the use of an appropriately chosen EWMA τ -chart appears to be a reasonable universal choice while a refined choice of the control chart can be done if the out-of-control scenario can be anticipated.

For future research, it could be investigated if an analogous approach for dependence monitoring is also possible for discrete-valued processes $(X_t)_{\mathbb{N}}$, such as a count process or ordinal process (Weiß 2018). Here, a possible idea could be to use the generalized ordinal patterns discussed by Schnurr and Fischer (2022), which explicitly allow for ties within the m -histories taken from $(X_t)_{\mathbb{N}}$. Furthermore, an OP-based monitoring of the cross-dependence of a multivariate process, in analogy to Schnurr and Dehling (2017), might be a promising research direction. Finally, a more general comparative study on dependence monitoring appears to be desirable, where also charts designed for late process changes should be compared to each other.

Supplementary Materials

Code and Data The file (supp_code.zip) contains the R-code `ARL0tau3_ooc_zs_AR005.r` (as well as the corresponding simulation output `ARL0tau3_ooc_zs_AR005.txt`), which generates a part of Table 2. All remaining simulation codes, which can be obtained from the corresponding author upon request, are simple modifications thereof. Furthermore, the R-code `ChemProcess.r` is included, which provides the dataset used for Section 6 together with all analyses.



Acknowledgments

The authors thank the associate editor and the referees for their useful comments on an earlier draft of this article.

Disclosure Statement

The authors report no conflict of interest.

ORCID

Christian H. Weiß  <http://orcid.org/0000-0001-8739-6631>
Murat Caner Testik  <http://orcid.org/0000-0003-2389-4759>

References

- Altioğlu, T., and Melamed, B. (2001), "The Case for Modeling Correlation in Manufacturing Systems," *IIE Transactions*, 33, 779–791. [340]
- Alwan, L. C. (1992), "Effects of Autocorrelation on Control Chart Performance," *Communications in Statistics — Theory and Methods*, 21, 1025–1049. [340]
- Alwan, L. C., and Roberts, H. V. (1988), "Time Series Modeling for Statistical Process Control," *Journal of Business and Economic Statistics*, 6, 87–95. [340]
- Atienza, O. O., Tang, L. C., and Ang, B. W. (1997), "ARL Properties of a Sample Autocorrelation Chart," *Computers and Industrial Engineering*, 33, 733–736. [340]
- Atienza, O. O., and Tang, L. C. (2006), "Simultaneous Monitoring of the Mean, Variance and Autocorrelation Structure of Serially Correlated Processes," in *Six Sigma*, eds. Tang, L. C., Goh, T. N., Yam, H. S., and Yoap, T., pp. 343–352, Chichester: Wiley. [340]
- Bagshaw, M., and Johnson, R. A. (1977), "Sequential Procedures for Detecting Parameter Changes in a Time-Series Model," *Journal of the American Statistical Association*, 72, 593–597. [340]
- Bandt, C. (2019), "Small Order Patterns in Big Time Series: A Practical Guide," *Entropy*, 21, 613. [341,342]
- Bandt, C., and Pompe, B. (2002), "Permutation Entropy: A Natural Complexity Measure for Time Series," *Physical Review Letters*, 88, 174102. [341,342]
- Beneke, M., Leemis, L. M., Schlegel, R. E., and Foote, B. L. (1988), "Spectral Analysis in Quality Control: A Control Chart based on the Periodogram," *Technometrics*, 30, 63–70. [340,348]
- Berger, S., Kravtsov, A., Schneider, G., and Jordan, D. (2019), "Teaching Ordinal Patterns to a Computer: Efficient Encoding Algorithms based on the Lehmer Code," *Entropy*, 21, 1023. [341]
- Box, G. E. P., and Jenkins, G. M. (1970), *Time Series Analysis: Forecasting and Control* (1st ed.), San Francisco: Holden-Day. [344,348]
- Caballero-Pintado, M. V., Matilla-García, M., and Ruiz Marín, M. (2019), "Symbolic Correlation Integral," *Econometric Reviews*, 38, 533–556. [341,342]
- Chakraborti, S., and Graham, M. A. (2019), "Nonparametric (Distribution-Free) Control Charts: An Updated Overview and Some Results," *Quality Engineering*, 31, 523–544. [341]
- Chakraborti, S., and Sparks, R. S. (2020), "Statistical Process Monitoring and the Issue of Assumptions in Practice: Normality and Independence," in *Distribution-Free Methods for Statistical Process Monitoring and Control*, eds. M. V. Koutras and I. S. Triantafyllou, pp. 137–155, Cham: Springer. [340,348]
- Davis, R. B., and Woodall, W. H. (1988), "Performance of the Control Chart Trend Rule under Linear Shift," *Journal of Quality Technology*, 20, 260–262. [343]
- Dooley, K. J., and Kapoor, S. G. (1990), "An Enhanced Quality Evaluation System for Continuous Manufacturing Processes, Part 1: Theory," *Journal of Engineering for Industry*, 112, 57–62. [340]
- Dürre, A., and Fried, R. (2020), "Robust Test for Detecting Changes in the Autocovariance Function of a Time Series," *Austrian Journal of Statistics*, 49, 35–45. [341]
- English, J. R., Lee, S.-C., Martin, T. W., and Tilmon, C. (2000), "Detecting Changes in Autoregressive Processes with \bar{X} and EWMA Charts," *IIE Transactions*, 32, 1103–1113. [341]
- Ermer, D. S., Chow, M. C., and Wu, S. M. (1979), "A Time Series Control Chart for a Nuclear Reactor," *Proceedings 1979 Annual Reliability and Maintainability Symposium*, pp. 92–98, New York: IEEE Press. [340]
- Gardner Jr., E. S. (1983), "Automatic Monitoring of Forecast Errors," *Journal of Forecasting*, 2, 1–21. [341,346]
- Hawkins, D. L. (1984), "Sequential Procedures for Detecting Deviations in the Parameters of the Autoregressive Model from Specified Targets," *Sequential Analysis*, 3, 121–154. [340]
- Hwang, H. B. (2005), "Simultaneous Identification of Mean Shift and Correlation Change in AR(1) Processes," *International Journal of Production Research*, 43, 1761–1783. [340]
- Jensen, W. A., Jones-Farmer, L. A., Champ, C. W., and Woodall, W. H. (2006), "Effects of Parameter Estimation on Control Chart Properties: A Literature Review," *Journal of Quality Technology*, 32, 395–409. [341]
- Jones-Farmer, L. A., Woodall, W. H., Steiner, S. H., and Champ, C. W. (2014), "An Overview of Phase I Analysis for Process Improvement and Monitoring," *Journal of Quality Technology*, 46, 265–280. [341]
- Keller, K., Sinn, M., and Emonds, J. (2007), "Time Series from the Ordinal Viewpoint," *Stochastics and Dynamics*, 7, 247–272. [341]
- Khakifirooz, M., Tercero-Gómez, V. G., and Woodall, W. H. (2021), "The Role of the Normal Distribution in Statistical Process Monitoring," *Quality Engineering*, 33, 497–510. [341]
- Knoth, S. (2006), "The Art of Evaluating Monitoring Schemes — How to Measure the Performance of Control Charts?" in *Frontiers in Statistical Quality Control 8*, eds. H.-J. Lenz and P.-T. Wilrich, pp. 74–99, Heidelberg: Physica-Verlag. [344,346]
- Knoth, S., and Schmid, W. (2004), "Control Charts for Time Series: A Review," in *Frontiers in Statistical Quality Control 7*, eds. H.-J. Lenz and P.-T. Wilrich, pp. 210–236, Heidelberg: Physica-Verlag. [340]
- Knoth, S., Tercero-Gómez, V. G., Khakifirooz, M., and Woodall, W. H. (2021), "The Impracticality of Homogeneously Weighted Moving Average and Progressive Mean Control Chart Approaches," *Quality and Reliability Engineering International*, 37, 3779–3794. [344]
- Koutras, M. V., and Triantafyllou, I. S. (2020), "Recent Advances on Univariate Distribution-Free Shewhart-Type Control Charts," in *Distribution-Free Methods for Statistical Process Monitoring and Control*, eds. M. V. Koutras and I. S. Triantafyllou, pp. 1–56, Cham: Springer. [341]
- Lawrance, A. J., and Lewis, P. A. W. (1981), "A New Autoregressive Time Series Model in Exponential Variables (NEAR(1)),," *Advances in Applied Probability*, 13, 826–845. [344]
- Li, J., Tsung, F., and Zou, C. (2014), "A Simple Categorical Chart for Detecting Location Shifts with Ordinal Information," *International Journal of Production Research*, 52, 550–562. [343]
- Montgomery, D. C. (2009), *Introduction to Statistical Quality Control* (6th ed.), New York: Wiley. [340,343,344]
- O'Donovan, T. M. (1983), *Short Term Forecasting: An Introduction to the Box-Jenkins Approach*, Chichester: Wiley. [348]
- Polunchenko, A. S., and Raghavan, V. (2018), "Comparative Performance Analysis of the Cumulative Sum Chart and the Shiryayev–Roberts Procedure for Detecting Changes in Autocorrelated Data," *Applied Stochastic Models in Business and Industry*, 34, 922–948. [340]
- Schnurr, A., and Dehling, H. (2017), "Testing for Structural Breaks via Ordinal Pattern Dependence," *Journal of the American Statistical Association*, 112, 706–720. [348]
- Schnurr, A., and Fischer, S. (2022), "Generalized Ordinal Patterns Allowing for Ties and their Applications in Hydrology," *Computational Statistics and Data Analysis*, 171, 107472. [348]
- Wang, J., Su, Q., and Xie, M. (2018), "A Univariate Procedure for Monitoring Location and Dispersion with Ordered Categorical Data," *Communications in Statistics — Simulation and Computation*, 47, 115–128. [343]
- Wardell, D. G., Moskowitz, H., and Plante, R. D. (1992), "Control Charts in the Presence of Data Correlation," *Management Science*, 38, 1084–1105. [340]
- Weiß, C. H. (2008), "Visual Analysis of Categorical Time Series," *Statistical Methodology*, 5, 56–71. [343]
- (2018), *An Introduction to Discrete-Valued Time Series*, Chichester: Wiley. [348]
- (2022), "Non-parametric Tests for Serial Dependence in Time Series based on Asymptotic Implementations of Ordinal-Pattern Statistics," *Chaos: An Interdisciplinary Journal of Nonlinear Science*, 32, 093107. [341,342,343,344]

- Weiß, C. H., Ruiz Marín, M., Keller, K., and Matilla-García, M. (2022), “Non-parametric Analysis of Serial Dependence in Time Series using Ordinal Patterns,” *Computational Statistics and Data Analysis*, 168, 107381. [341]
- Ye, N., Masum, S., Chen, Q., and Vilbert, S. (2002), “Multivariate Statistical Analysis of Audit Trails for Host-based Intrusion Detection,” *IEEE Transactions on Computers*, 51, 810–820. [343]
- Yourstone, S. A., and Montgomery, D. C. (1989), “A Time-Series Approach to Discrete Real-Time Process Quality Control,” *Quality and Reliability Engineering International*, 5, 309–317. [340]
- (1991), “Detection of Process Upsets—Sample Autocorrelation Control Chart and Group Autocorrelation Control Chart Applications,” *Quality and Reliability Engineering International*, 7, 133–140. [340]